5734

The importance of optical pathlength control for plasma absorption measurements

Brett A Cruden and M V V S Rao

Eloret Corporation

Surendra P Sharma and M Meyyappan

NASA Ames Research Center

An inductively coupled GEC Cell with modified viewing ports has been used to measure in-situ absorption in CF_4 plasmas via Fourier Transform Infrared Spectroscopy, and the results compared to those obtained in a standard viewport configuration. The viewing ports were modified so that the window boundary is inside, rather than outside, of the GEC cell. Because the absorption obtained is a spatially integrated absorption, measurements made represent an averaging of absorbing species inside and outside of the plasma. This modification is made to reduce this spatial averaging and thus allow a more accurate estimation of neutral species concentrations and temperatures within the plasmas. By reducing this pathlength, we find that the apparent CF_4 consumption increases from 65% to 95% and the apparent vibrational temperature of CF_4 rises by 50-75 K. The apparent fraction of etch product SiF_4 decreases from 4% to 2%. The data suggests that these density changes may be due to significant temperature gradients between the plasma and chamber viewports.

52.70.Kz, 82.33.Xj, 82.80.Gk, 07.57.Ty

In a previous article, we reported Fourier Transform Infrared (FTIR) spectroscopy measurements of an inductively coupled CF_4 plasma.[1] In this article, we also discussed many of the limitations and approximations of the FTIR technique that are well documented, though often overlooked, in the literature. These problems apply to other broadband absorption techniques as well as FTIR. One particularly important problem in any absorption technique is the effect of spatial variations on extracting averaged quantities out of the absorption data. Absorption occurs everywhere along the path of the light, and this path typically includes not only the plasma, but also the region outside of the plasma and the viewport regions. The result is an absorption measurement that is an average of the absorptions in the plasma, in the viewport and regions in between. However, what is really of interest is the absorption in the plasma. The concentrations and temperatures in the viewport region will generally differ from those in the plasma, often significantly. In this work, the effect of the pathlength is examined by changing the spacing between viewing windows and comparing these results.

Figure 1 shows the configuration of the GEC Cell with and without the modified windows. Without the modified windows, the absorption pathlength was 58.4 cm and included 33 cm of viewport space. The redesigned viewport window sticks into the GEC Cell so that the absorption pathlength now becomes 20.3 cm. The window is still far enough removed from the plasma that it is not expected to create significant perturbation of the plasma. However, an increase in reflected power is observed in the modified configuration. The plasma is created over an electrode space of 10 cm diameter, but

extends further beyond this edge. The plasma density drops significantly on the outer edges of the electrode and extends somewhat beyond the electrode edge. Thus, while the plasma may have a denser "core" of about 4-6 cm in diameter, it could be thought of as having a diameter of the order of 10-12 cm.[2] The spatially averaged quantities obtained from this modified reactor should therefore be more representative of the actual concentrations in the plasma, although it will still contain some area of "cold" gas outside of the plasma.

There are, however, some problems associated with placing the windows near the plasma in this fashion. Because the windows are near the plasma, they are more liable to interact with the plasma. This means that the windows may be etched or plasma deposited films will grow on them over time, altering their transmission properties. To help with this problem, the windows were designed with stainless steel shutters that can block the windows from the plasma when the FTIR is not in use. Another serious problem is heating of the windows by the plasma. In the original design, with the windows so far removed from the plasma, they remained at room temperature during experiments. With the windows near the plasma, however, they can heat up significantly. To reduce the risk of cracking of the windows during this plasma-induced thermal cycling, NaCl windows were used instead of KBr windows. Another problem exists with "channeling," or the multiple internal reflections of the IR beam within the viewport window.[3] Even with NaCl's high transmittance, or with an antireflective coating, this effect is still present to some degree. In most experiments, the properties of the window do not change during processing, so the channeling noise cancels out when the absorbance is calculated.

However, the plasma heating causes a change in window thickness and transmittance properties so that the channeling noise is different between the background and sample scans. The result is a high frequency noise that limits the signal to noise attainable in a high resolution spectrum. Therefore, these experiments are all performed with a 1 cm^{-1} resolution. There is still some fluctuation of the baseline due to changing window properties that is not easily corrected for, however this fluctuation is generally considerably less than the magnitude of absorption. Measurement of absorbance following the plasma process permits subtraction of signal due to permanent changes in the window caused by the plasma (i.e. etching or deposition.)

Other than the modification of the viewport windows, the experimental set up and procedure is similar to that in our previous work[1] with a few changes. The matching network has been modified as described in Ref. 4 and the power supply is an Advanced Energy RFX-600. A change in mass flow controllers and pumping configuration required that the CF_4 flow rate be reduced to 10 sccm. The CF_4 plasma is run for a few hours to allow for chamber conditioning[4] and heating before any data is collected. Because these changes in operating conditions and equipment can alter the plasma properties, the experiments for both viewport configurations were repeated in this work. A power setting of 300 W is used, and pressure is varied from 10-50 mtorr. The reflected power was typically in the range of 7-10 W for this forward power. Under these conditions, the estimated CF_4 fraction is reduced by about 15% over the results of our previous work,[1] indicating that the reduction in flow rate (or, increased residence time) plays a role in determining the steady state concentrations in the system.

The CF_4 absorption spectrum for the two different window configurations, corrected for the different pathlengths, is shown in Figure 2(a). It is readily apparent that significantly more CF_4 absorption is observed with the longer pathlength configuration, suggesting there is an abundance of CF_4 within the viewport region relative to the plasma. As described in Ref. 1, absorption due to CF_4 is removed from the spectrum by subtracting absorption cross-sections determined from measurements with the GEC Cell filled with CF_4 to pressures between 1 and 50 mtorr, without the plasma on. After this subtraction, there is an absorption remaining that is not well characterized by CF_4. (Figure 2(b)) This remaining absorption is of a similar shape and magnitude regardless of the window position, suggesting it is due to species present primarily in the plasma, and not the viewport region. The differences between the two cases are generated in the analysis because the residual spectrum and CF_4 spectrum do not add linearly, as described briefly in Ref. 1. This effect is most pronounced in the higher absorbance cases of the original configuration. In our previous publication, we attributed this absorption to excited vibrational states of CF_4, while the rotational excitation is not detected because of absorption averaging with the cold CF_4 in the viewport.[1] This was assumed to be the reason because the shoulder region does not agree well with a simulated CF_3 spectrum. This same shoulder has been previously attributed to CF_3 absorption,[5] though other workers have independently drawn conclusions identical to ours based on comparison to unpublished experimental results.[6]

The estimated mole fraction of CF_4, due to both undissociated parent gas and recombination products, is shown in Figure 3(a) for both window configurations. This data has not been corrected for spatial variations in the concentration or gas temperature. Also shown is the apparent fraction of gas due to the unidentified residual spectrum seen in Figure 2(b). An upper and lower limit for this value is determined by using the integrated absorption coefficients for room temperature CF_4 (this work) and CF_3 (Ref. 5), respectively. These limits are noted by the error bars in Figure 3(b). With the exception of the 30 mtorr case, which is anomalously large, this residual absorption can account for ~52% of the gas present. The apparent fraction of cold CF_4 remaining is considerably less when the modified viewport is used, suggesting that significant amounts of cold CF_4 are present in the viewport. The residual area accounts for a much greater fraction of the gas when the modified configuration is used because its absorption occurs primarily within the plasma, and the effective absorption length for this part of the spectrum is not well represented by the window spacing. It is noteworthy that the unheated CF_4 fraction at 10 mtorr is consistently a few percent greater than in the higher pressure cases, regardless of the window configuration.

In our previous publication,[1] COF_2, CO and SiF_4 were all observed from etching of the quartz coupling window. The CO and COF_2 peaks are not identifiable in the modified viewport configuration because of the increased noise level and lower resolution. A broad absorption in the vicinity of the SiF_4 peak is observed with the modified window configuration (Figure 4(a)), but lacks the structure characteristic of the SiF_4 absorption seen with the larger window spacing. This absence of structure may indicate a high

temperature SiF_4 where the structure is washed out completely by hot bands. The relative concentrations of SiF_4 are shown in Figure 4(b). As with CF_4, significantly more SiF_4 is observed when a longer pathlength is used, and a shoulder region is observed of comparable shape and intensity for both configurations. The case with SiF_4 is analogous with that of CF_4, where cold SiF_4 can be formed by recombination on the wall. The lower abundance of SiF_4 inside the plasma may indicate that SiF_x radicals (x = 1-3) may serve as the primary etch products.

The vibrational temperature of CF_4 can be estimated from the ratio of the fundamental and hot band peaks.[1,7] In this case, we were not able to use the second hot band because its intensity was too weak at this resolution. The results of the temperature fit using the fundamental and first hot band for both window configurations is shown in Figure 5. By simply changing the absorption pathlength, the apparent vibrational temperature has risen by between 50-75 K. However, this is done with approximately 40% of the absorption path being outside of the plasma, where the CF_4 concentration is highest. It is probable that this temperature is still much less than the actual neutral temperature in the plasma. A general trend of increasing temperature with pressure is observed. This variation is consistent with model predictions results of this system, where the elevated temperature is due primarily to exothermic neutral recombination reactions.[8] As pressure increases, the neutral reaction rate increases giving a higher temperature with pressure. The rotational temperature, however, does not appear greatly changed, even with this improved viewport configuration, as the reference CF_4 spectrum fits the Q and R branches of the spectrum fairly well.

The elevated neutral temperature in the plasma will result in an overestimate of the neutral density in the plasma. Because absorption spectroscopy measures the number density, regardless of the gas temperature, the calculated mole fraction will be underestimated in this work. This may explain why lower concentrations of both CF_4 and SiF_4 are observed when the absorption path is shortened. The higher neutral temperature will result in a lower density inside the plasma. If one considers the ideal gas law, a neutral temperature of 500 K within the plasma, as has been predicted in a model of this system,[8] will mean the total density within the plasma is three-fifths of that within the viewport. If this were the case, one would estimate CF_4 and SiF_4 fractions near 13% and 4%, respectively. The residual absorption underlying CF_4 appears to be the major species within the plasma. Without a temperature or pathlength correction, and assuming a cross-section similar to that of CF_3 or CF_4, it accounts for over 50% of the gas in the system. Once these corrections are made, it can account for the entirety of the gas. However, these corrections cannot be accurately made because the temperature, concentration profile, and actual absorption cross-section, are not accurately known.

In conclusion, we have demonstrated very important differences in the absorption spectrum obtained under different viewport configurations in an inductively coupled CF_4 plasma. Strong spatial variations between the plasma and chamber viewports result in a significant overestimate of stable neutral species (e.g. CF_4 and SiF_4) concentrations in the plasma and an underestimate of the temperature within the plasma. This overestimate is likely due to thermal gradients between the plasma and viewport. Insufficient knowledge

of the plasma neutral temperature makes it difficult to accurately assess the number fraction of these species in the plasma. The spectra obtained for both SiF_4 and CF_4 lack the structure characteristic of absorption by these species, which may be due to a large population of excited vibrational states.

[1] B. A. Cruden, M. V. V. S. Rao, S. P. Sharma, and M. Meyyappan, Plasma Sources Sci. Technol., submitted (2001).

[2] M. V. V. S. Rao, S. P. Sharma, B. A. Cruden, and M. Meyyappan, Plasma Sources Sci. Technol., submitted (2001).

[3] P. R. Griffiths and J. A. de Haseth, *Fourier Transform Infrared Spectroscopy*, Vol. 83 (John Wiley & Sons, New York, 1986).

[4] B. A. Cruden, M. V. V. S. Rao, S. P. Sharma, and M. Meyyappan, JVST B, submitted (2001).

[5] M. J. Goeckner, M. A. Henderson, J. A. Meyer, and R. A. Breun, J Vac Sci Technol A **12**, 3120-3125 (1994).

[6] I. C. Abraham, Ph. D. Thesis, University of Wisconsin -- Madison, 1999.

[7] M. Haverlag, F. J. de Hoog, and G. M. W. Kroesen, Journal of Vacuum Science & Technology A **9**, 327-330 (1991).

[8] D. B. Hash, D. Bose, M. V. V. S. Rao, B. A. Cruden, M. Meyyappan, and S. P. Sharma, J Vac Sci Technol A, in press (2001).

Figure 1. Schematic of the GEC Cell viewports. On the left is shown the original viewport design, on the right is the modified viewport design. Other viewports on the GEC Cell are omitted for clarity.

Figure 2. Absorbance measurements for 50 mtorr, 300 W CF_4. (a) Overall absorbance, divided by pathlength to give a spatially averaged absorbance. The distinct peaks near 1280 cm^{-1} are characteristic of CF_4. (b) Absorbance after subtraction of the CF_4 signal, without pathlength correction. The magnitude and shape of this remaining background absorbance is similar in both configurations.

Figure 3. (a) Apparent fraction of CF_4 remaining in both viewport configurations. Significantly less CF_4 is seen in the modified configuration, suggesting large concentration gradients. (b) Apparent fraction of the gas due to the residual spectrum underlying CF_4. The error bars are estimated by applying the absorption coefficients of CF_3 and CF_4 in this region.

Figure 4. (a) SiF_4 absorption, divided by pathlength, in each viewport configuration, and (b) the apparent density associated with each. This data shows evidence for significant gradients in concentration with there being more SiF_4 within the viewport regions.

Figure 5. Plot of apparent vibrational temperature of CF_4 versus pressure for both viewport configurations. It is apparent that a larger temperature is measured when the viewport regions are excluded

Figure 1

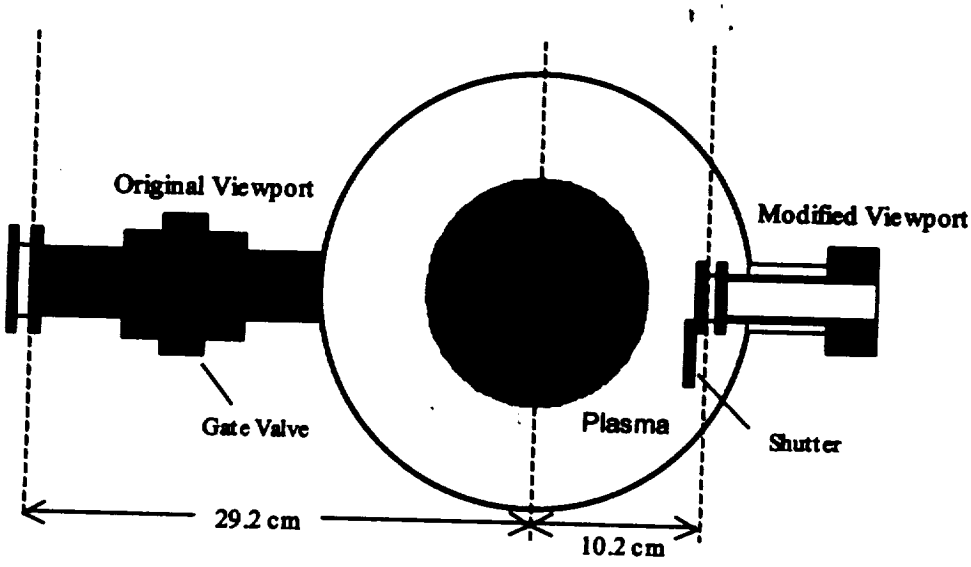
Original Viewport
Modified Viewport
Gate Valve
Plasma
Shutter
29.2 cm
10.2 cm

Figure 2

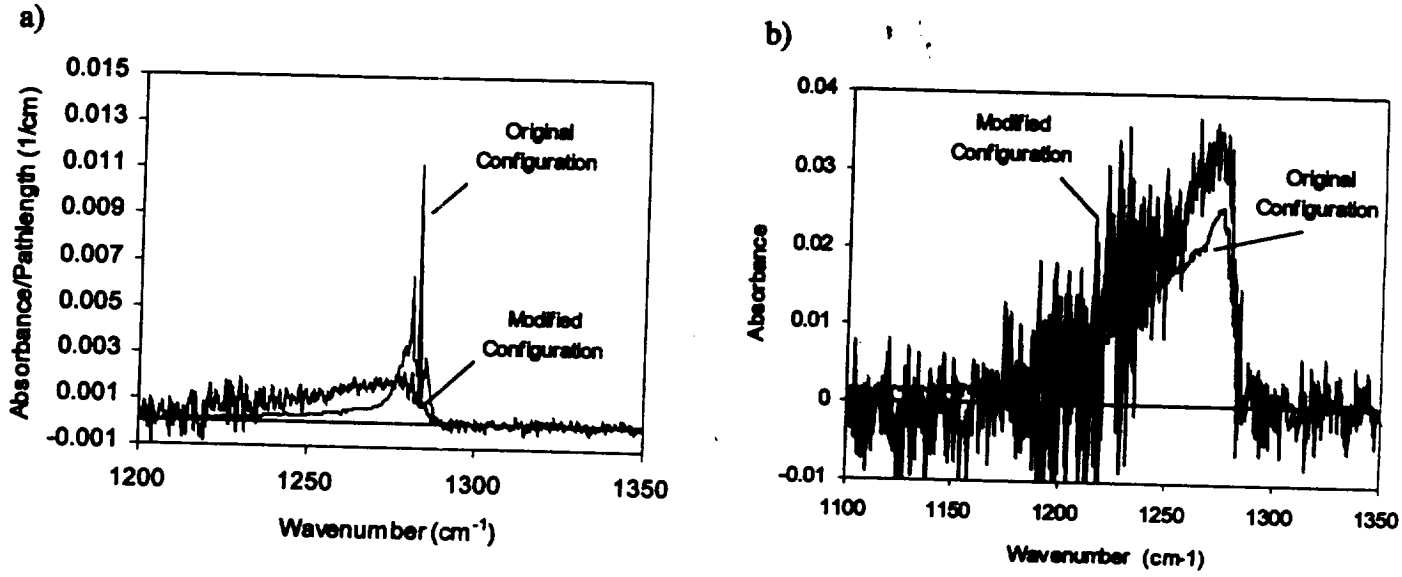
a)
0.015
0.013
0.011
0.009
0.007
0.005
0.003
0.001
-0.001
Absorbance/Pathlength (1/cm)
Original Configuration
Modified Configuration
1200
1250
1300
1350
Wavenumber (cm-1)
b)
0.04
0.03
0.02
0.01
0
-0.01
Absorbance
Modified Configuration
Original Configuration
1100
1150
1200
1250
1300
1350
Wavenumber (cm-1)

Figure 3

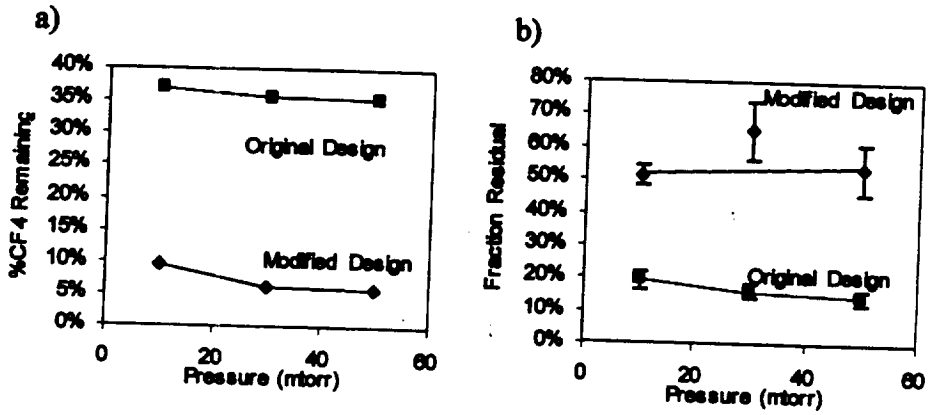
a)
40%
35%
30%
25%
20%
15%
10%
5%
0%
%CF4 Remaining
Original Design
Modified Design
0
20
40
60
Pressure (mtorr)
b)
80%
70%
60%
50%
40%
30%
20%
10%
0%
Fraction Residual
Modified Design
Original Design
0
20
40
60
Pressure (mtorr)

Figure 4

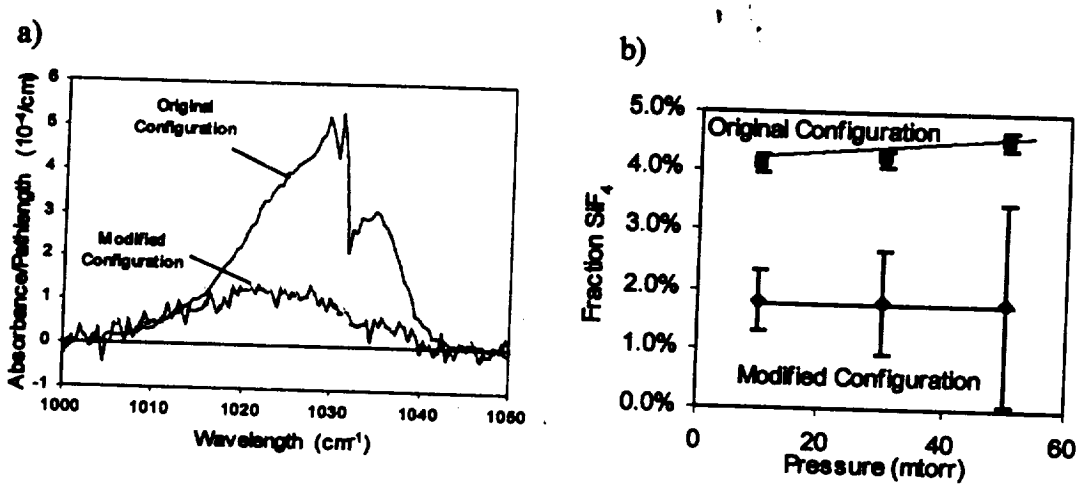
a)
Original Configuration
Modified Configuration
Absorbance/Pathlength (10⁻⁴/cm)
Wavelength (cm⁻¹)
b)
Original Configuration
Modified Configuration
Fraction SiF4
Pressure (mtorr)

Figure 5

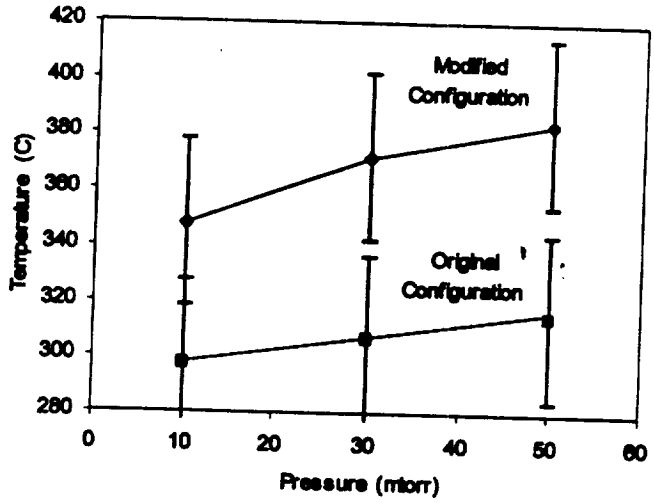
420
400
380
360
340
320
300
280
Temperature (C)
0
10
20
30
40
50
60
Pressure (mtorr)
Modified
Configuration
Original
Configuration